Molecular Plant Pathology

MOLECULAR PLANT PATHOLOGY (2012) **13**(7), 677–689 DOI: 10.1111/J.1364-3703.2011.00779.X

MoSwi6, an APSES family transcription factor, interacts with MoMps1 and is required for hyphal and conidial morphogenesis, appressorial function and pathogenicity of *Magnaporthe oryzae*

ZHONGQIANG QI[1,†], QI WANG[1,†], XIANYING DOU[1], WEI WANG[1], QIAN ZHAO[1], RUILI LV[1], HAIFENG ZHANG[1], XIAOBO ZHENG[1], PING WANG[2] AND ZHENGGUANG ZHANG[1,*]

[1]*Department of Plant Pathology, College of Plant Protection, Nanjing Agricultural University, and Key Laboratory of Integrated Management of Crop Diseases and Pests, Ministry of Education, Nanjing 210095, China*

[2]*The Research Institute for Children and Department of Pediatrics, Louisiana State University Health Sciences Center, New Orleans, LA 70118, USA*

SUMMARY

The *Magnaporthe oryzae* mitogen-activated protein kinase (MAPK) MoMps1 plays a critical role in the regulation of various developmental processes, including cell wall integrity, stress responses and pathogenicity. To identify potential effectors of MoMps1, we characterized the function of MoSwi6, a homologue of *Saccharomyces cerevisiae* Swi6 downstream of MAPK Slt2 signalling. MoSwi6 interacted with MoMps1 both *in vivo* and *in vitro*, suggesting a possible functional link analogous to Swi6–Slt2 in *S. cerevisiae*. Targeted gene disruption of *MoSWI6* resulted in multiple developmental defects, including reduced hyphal growth, abnormal formation of conidia and appressoria, and impaired appressorium function. The reduction in appressorial turgor pressure also contributed to an attenuation of pathogenicity. The *ΔMoswi6* mutant also displayed a defect in cell wall integrity, was hypersensitive to oxidative stress, and showed a significant reduction in transcription and activity of extracellular enzymes, including peroxidases and laccases. Collectively, these roles are similar to those of MoMps1, confirming that MoSwi6 functions in the MoMps1 pathway to govern growth, development and full pathogenicity.

INTRODUCTION

Magnaporthe oryzae, the causal agent of rice blast, has been studied extensively as a model organism for the investigation of plant diseases because of its economic and social significance, and its experimental tractability (Caracuel-Rios and Talbot, 2007; Ebbole, 2007; Talbot, 2003; Valent *et al*., 1991). The infectious structure, the appressorium, has a chitin-rich differentiated cell wall and contains a distinct layer of melanin surrounding the cell membrane, which acts as a barrier to the efflux of solute that occurs during turgor generation (Henson *et al*., 1999). Turgor translates into mechanical force, enabling the emerging penetration peg to force through the leaf cuticle. On entry, the fungal hyphae invade the plant tissue to cause blast disease (Talbot, 2003).

In *M. oryzae*, the formation of a penetration peg from the base of the appressorium requires the MoMps1 mitogen-activated protein kinase (MAPK) signal transduction pathway, which is analogous to the Slt2 MAPK-mediated cell wall integrity pathway of the budding yeast *Saccharomyces cerevisiae* (Xu *et al*., 1998). MoMps1, a functional homologue of the *S. cerevisiae* protein kinase Slt2, is necessary for functional appressorium formation and successful plant infection (Xu *et al*., 1998). MoMck1, an *S. cerevisiae* MAPK kinase kinase (MAPKKK) homologue, is also necessary for appressorium function (Jeon *et al*., 2008). In addition, the *S. cerevisiae* Slt2 signalling pathway targets the MADS-box transcription factor Rlm1 (Watanabe *et al*., 1997), and a *ΔMomig1* mutant lacking an Rlm1 homologue, MoMig1, forms hypha-like structures on artificial surfaces, but is unable to cause blast disease (Mehrabi *et al*., 2008). In addition to Rlm1, the transcription factors downstream of Slt2 also include Swi4 and Swi6, which link cell wall biogenesis to cell cycle regulation in *S. cerevisiae* (Iyer *et al*., 2001). Moreover, the yeast Slt2 pathway also regulates the response to oxidative stress (Krasley *et al*., 2006).

The APSES (Asm1, Phd1, Sok1, Efg1 and StuA) family of fungal transcription factors regulates gene expression for a diverse array of functions, including morphological transitions, expression of metabolic and secreted enzymes and cell wall proteins, and cellular signalling in *S. cerevisiae*; Phd1 and Sok2 regulate pseudohyphal growth as an activator and repressor, respectively (Cid *et al*., 1995; Levin, 2005; Ward *et al*., 1995). In *Candida albicans*, Efg1 controls the induction of hyphal growth, white–opaque switching and chlamydospore formation (Tebarth *et al*., 2003), whereas Efh1 supports the regulatory function of Efg1 (Doedt *et al*., 2004). In *Aspergillus fumigatus*, deletion mutants of *STUA* result in the formation of abnormal conidiophores (Sheppard *et al*., 2005), whereas the deletion mutant of *ASM1* shows slow germination

**Correspondence*: Email: zhgzhang@njau.edu.cn
†These authors contributed equally to this work.

and mycelial growth in *Neurospora crassa* (Aramayo *et al*., 1996). The *Glomerella cingulata* StuA homologue GcStuA is involved in the maintenance of appressoria turgor pressure and is required for full pathogenicity (Tong *et al*., 2007). Similarly, the *M. oryzae* StuA homologue Mstu1 is required for the efficient mobilization of conidial reserves during appressorial turgor generation. However, Mstu1 is indispensable for pathogenicity (Nishimura *et al*., 2009). The last finding suggests that the diverse roles of the APSES transcription factors are also differentiated. Finally, as the cyclic adenosine monophosphate (cAMP) and MAPK signal transduction pathways are central to infection-related development in all pathogenic fungi studied, APSES transcription also serves as a target of cAMP signalling (D'Souza and Heitman, 2001; Tucker and Talbot, 2001).

The characterization of MoMps1 downstream targets will promote a better understanding of the MoMps1 pathway contributing to the development and pathogenesis of *M. oryzae*. In this article, we characterize MoSwi6 as an APSES transcription factor that is downstream of MoMps1 signalling. Our results postulate that *M. oryzae* has evolved a distinct downstream transcription factor in the conserved MAPK cascade in comparison with *S. cerevisiae*.

RESULTS

Sequence analysis of MoSwi6

The predicted transcription factor MoSwi6 corresponds to the *M. oryzae* MGG_09869.6 locus with an open reading frame (ORF) of 806 amino acids, which is interrupted by two introns. Southern hybridization analysis revealed that *MoSWI6* is a single gene (Fig. S1, see Supporting Information). Comparison of Swi6 homologous proteins from various organisms revealed that MoSwi6 shares a high level of similarity with those of ascomycetous fungi, including *Gibberella zeae* (XP_384396), *Podospora anserina* (XP_001903283) and *N. crassa* (XP_962967), but is more distant from *S. cerevisiae* Swi6 (NP_013283) (Fig. S2, see Supporting Information).

The predicted MoSwi6 protein contains two conserved domains. One is an N-terminal APSES DNA-binding domain and the other is an ankyrin repeat (ANK repeat) domain located at the C-terminus. Sequence alignment analysis revealed that the APSES domain is well conserved among the filamentous fungi (Fig. S3A, see Supporting Information), whereas the ANK repeat with the conserved L-region is specific to and shared by both filamentous fungi and *S. cerevisiae* (Fig. S3B).

MoSwi6 interacts with MoMps1

In *S. cerevisiae*, the MAPK Mpk1 protein regulates the functions of Swi6. As MoMps1 (MGG_04943.6) is the functional homologue of yeast Mpk1 in *M. oryzae*, which contains conserved domains, such as the binding domain (MBF) and the kinase domain (Xu *et al*., 1998), we examined the interaction between MoSwi6 and MoMps1 initially through yeast two-hybrid assay. As shown in Fig. 1A, yeast host cells transformed with both MoSwi6 and MoMps1 grew on both permissive and selective media. In contrast, yeast expressing either MoSwi6 or MoMps1 failed to grow on selective medium. Control strains expressing the strongly interacting pGADT7-RecT and pGBKT7-53 or the noninteracting pGADT7-RecT and pGBKT7-Lam were included as positive and negative controls, respectively.

To confirm the interaction between MoSwi6 and MoMps1, co-immunoprecipitation (co-IP) was performed. The *MoMPS1*-3 x FLAG and *MoSWI6*-GFP (GFP, green fluorescent protein) constructs were generated (see Materials and methods) and co-transformed into the wild-type strain 70-15. Transformants expressing the *MoMPS1*-3xFLAG and *MoSWI6*-GFP constructs

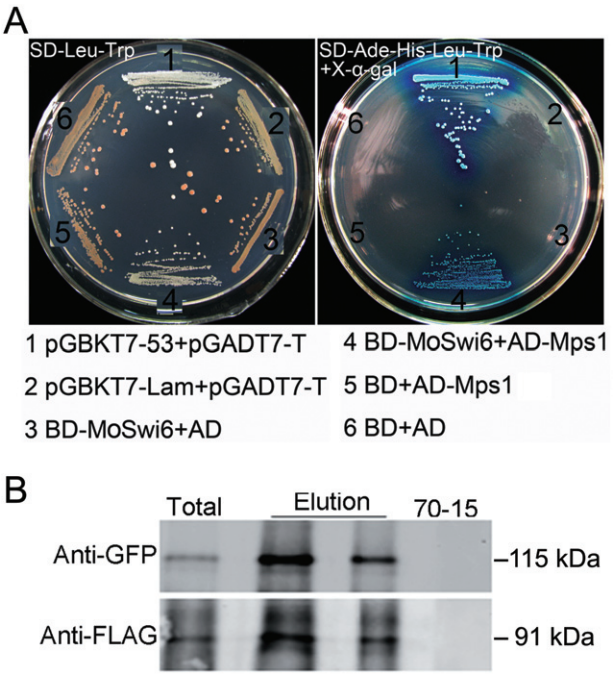

Fig. 1 MoSwi6 interacts with MoMps1. (A) A yeast two-hybrid assay was used to examine the interaction between MoSwi6 as a bait and MoMps1 as a prey. The interaction between pGBKT7-53 and pGADT7-T was used as the positive control, and noninteractions between pGBKT7-Lam and pGADT7-T, BD (pGBKT7)-MoSwi6 and AD (pGADT7), BD and AD-MoMps1, and empty AD and BD vectors were used as negative controls. Plates were incubated at 30 °C for 3 days before being photographed. (B) Co-immunoprecipitation assay for the interaction of MoSwi6 with MoMps1. Western blot analysis with total proteins (Total) isolated from transformants co-expressing the *MoSWI6*-GFP and *MoMPS1*-3xFLAG constructs and proteins eluted from the anti-FLAG M2 beads (Elution). The presence of MoSwi6 and MoMps1 was detected with an anti-GFP and an anti-FLAG antibody, respectively. GFP, green fluorescent protein.

were identified by polymerase chain reaction (PCR) and confirmed by Western blot analysis with an anti-FLAG antibody. When detected with an anti-GFP antiserum, a 115-kDa protein band of the expected size of MoSwi6 was found. In proteins eluted from anti-FLAG M2 beads, the same protein band was detected with the anti-GFP antibody (Fig. 1B). These results suggest that MoSwi6 might have a potential role in controlling the developmental processes mediated by MoMps1.

MoSWI6 gene disruption and Δ*Moswi6* mutant complementation

Gene-targeted replacement was used to investigate the function of MoSwi6. Following the methods described by Zhang *et al*. (2009), putative transformants were selected from complete medium (CM) containing hygromycin B (300 μg/mL), and verified by PCR amplification and Southern blotting analysis (Fig. S4B,C, see Supporting Information). Further confirmation of two Δ*Moswi6* mutants was obtained by reverse transcriptase-polymerase chain reaction (RT-PCR) to amplify fragments within the deleted region of the *MoSWI6* gene. As expected, no transcription products were amplified from the Δ*Moswi6* mutants (Fig. S4D). In addition, a Δ*Moswi6/MoSWI6* complementation strain was created by reintroducing the *MoSWI6* gene sequence containing the native promoter.

Δ*Moswi6* mutant shows abnormal hyphae as a result of altered chitin synthesis and compromised melanization

We evaluated the vegetative growth of the Δ*Moswi6* mutant on medium including CM, V8, oatmeal and SDC (100 g rice straw decoction into 1 L double-distilled H_2O, 40 g cornmeal and 15 g agar) (Dou *et al*., 2011; Song *et al*., 2010). The mutants exhibited reduced radial growth and less pigmentation in hyphae on all media compared with the wild-type strain Guy11 (Fig. S5, see Supporting Information). In addition, mycelia of the Δ*Moswi6* mutant were more inflated than those of Guy11 (Fig. 2A,B, see arrows), particularly at the hyphal tips (Fig. 2C,D). In *S. cerevisiae*, the APSES transcription factors are well-known cellular development and differentiation regulators (Watanabe *et al*., 1997). Changes in APSES expression of filamentous fungi could be correlated with changes occurring in the nuclei (Wang and Szaniszlo, 2007). However, no abnormal nuclei were found in the Δ*Moswi6* mutant following 4,6-diamino-2-phenylindole (DAPI) staining (Fig. 2E,F, see arrows).

The fungal cell wall plays an essential role in maintaining hyphal morphology and adaptation to the environment. To test whether the inflated hyphae of the Δ*Moswi6* mutant were a result of changes in the cell wall structure, a variety of cell wall-perturbing agents, including inhibitors and osmotic stressors, were

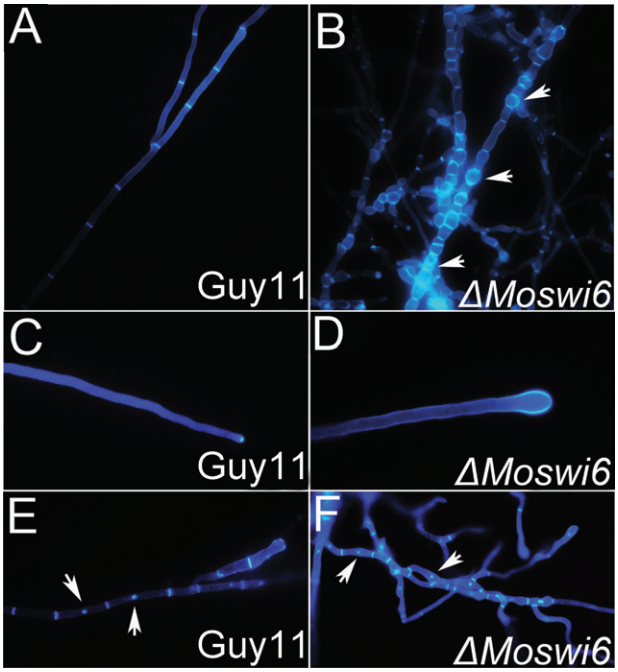

Fig. 2 *MoSWI6* deletion results in altered hyphal morphology. Morphology was determined microscopically after the Δ*Moswi6* mutants and the wild-type strains had been grown for 2 days on complete medium (CM)-overlaid microscope slides. Hyphae were stained with calcofluor white for chitin distribution. Fluorescence indicative of chitin was mainly distributed on the apex of hyphae and septa. (A, B) The Δ*Moswi6* mutant hyphae showed swelling and became more flexible. (C, D) The tips of the Δ*Moswi6* mutant hyphae showed expansive growth. (E, F) After staining with both 4,6-diamino-2-phenylindole (DAPI) and calcofluor white, no changes were found between the nuclei of the Δ*Moswi6* mutants and the wild-type strain.

used. The Δ*Moswi6* mutants showed increased resistance to calcofluor white (200 μg/mL), sodium dodecylsulphate (SDS) (0.01%, w/v) and sorbitol (1 M) relative to Guy11 (Fig. 3A; Table S1, see Supporting Information). As chitin is one of the main integrity components of the fungal cell wall (Roncero, 2002), the chitin content was estimated following the method described by Song *et al*. (2010). The Δ*Moswi6* mutant had a higher chitin content than the wild-type Guy11 and the complemented (Δ*Moswi6*/*MoSWI6*) strains (Fig. 3B). In addition, as chitin synthesis is dependent on the activity of chitin synthase enzymes, which catalyse the formation of chitin from uridine diphosphate *N*-acetylglucosamine (UDP-GlcNAc) (Odenbach *et al*., 2009), we analysed the expression of several chitin synthases using quantitative RT-PCR (Fig. 3C). The result consistently suggested that the expression of several chitin synthase genes was increased significantly in the Δ*Moswi6* mutant.

Reduced pigmentation of the Δ*Moswi6* mutant suggested that melanin biosynthesis might be compromised. We thus analysed the transcript abundance of the *MoBUF1* (MGG_02252) and *MoRSY1* (MGG_05059) genes involved in melanin biosynthesis

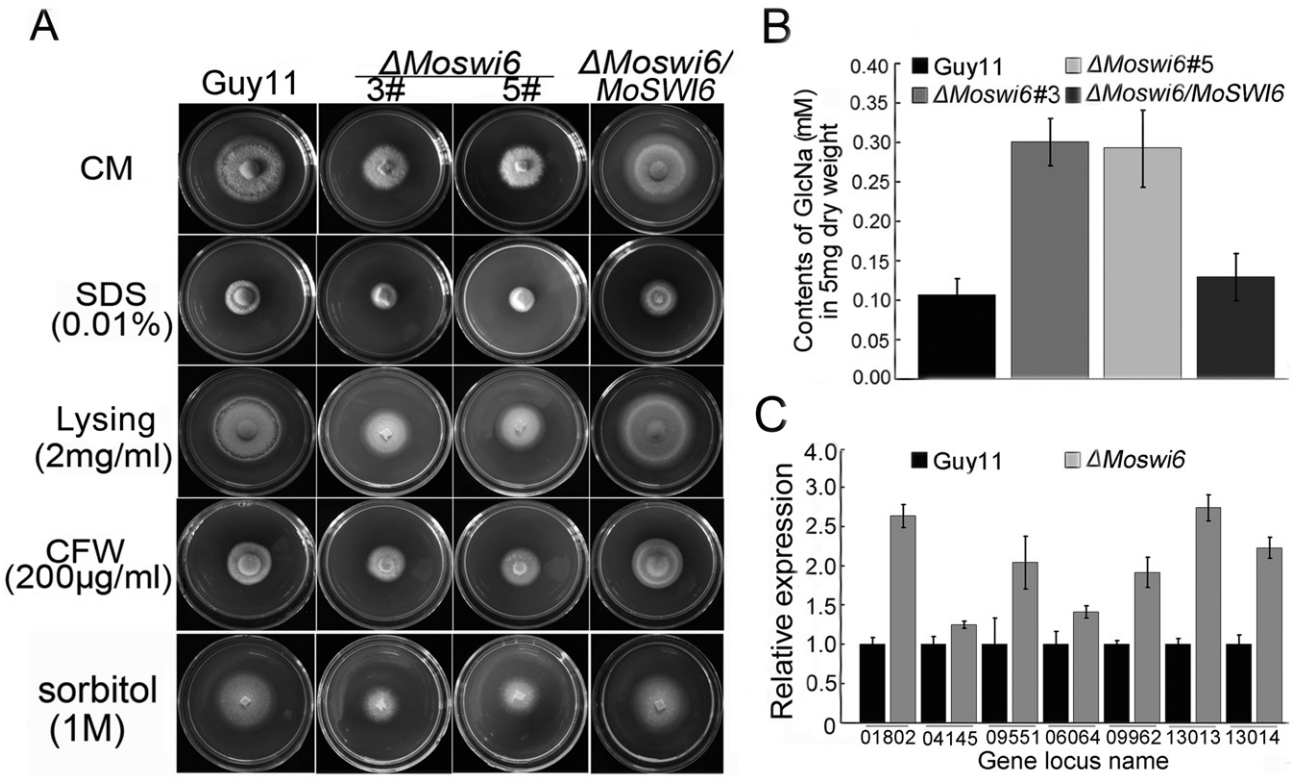

Fig. 3 Δ*Moswi6* mutants exhibit altered tolerance to various stress inducers related to the cell wall and membrane stress functions. (A) The Guy11, Δ*Moswi6* mutants (#3 and #5) and reconstituted (Δ*Moswi6/MoSWI6*) strains were incubated on complete medium (CM) supplemented with 0.01% sodium dodecylsulphate (SDS), 2 mg/mL lysing enzyme, 200 μg/mL calcofluor white (CFW) or 1 M sorbitol at 28 °C for 6 days before being photographed. Δ*Moswi6* was tolerant to the cell membrane stressors. (B) Determination of GlcNac using the fluorometric Morgan–Elson method. The chitin content was increased in the Δ*Moswi6* mutant relative to the wild-type. The GlcNac contents of the Δ*Moswi6* mutant and wild-type strains were tested with 5 mg of dry weight hyphae. The newly released reducing terminal *N*-acetylglucosamine (GlcNAc) in the supernatant was detected by fluorescence with a Nanodrop-1000 fluorescence spectrophotometer at a wavelength of 585 nm. Standard curves were prepared from stocks of 0.05–0.4 mM GlcNAc. Data represent three independent experiments, each performed three times. (C) Quantitative reverse transcriptase-polymerase chain reaction (RT-PCR) transcription analysis of chitin synthase expression in the Δ*Moswi6* (#3) mutant and Guy11. The seven chitin synthase genes are MGG_01802, MGG_04145, MGG_0955, MGG_06064, MGG_09962, MGG_13013 and MGG_13014. The Δ*Moswi6* (#5) mutant showed similar results and the data represent three independent experiments, each performed three times.

using quantitative RT-PCR. Consistent with reduced pigmentation, the expression of *MoBUF1* and *MoRSY1* was reduced significantly in the Δ*Moswi6* mutant (Fig. S6, see Supporting Information). Furthermore, we found that exogenous copper sulphate ($CuSO_4$) restored melanization to the Δ*Moswi6* mutant (Fig. 4A, see arrows). As Cu^{2+} stimulates melanization through increased laccase activity (Skamnioti *et al*., 2007), we compared the laccase activities between the Δ*Moswi6* mutant and control strains by measuring the oxidation of the laccase substrate 2,2′-azino-di-3-ethylbenzathiazoline-6-sulphonate (ABTS, Sigma, A1888, St. Louis, MO, USA) (Shindler *et al*., 1976). Indeed, laccase activity was reduced in the Δ*Moswi6* mutant (Fig. 4B, panel a), which was recovered by the addition of $CuSO_4$ (Fig. 4B, panels b–g). The detection of culture filtrates showed similar reductions in laccase activity for the Δ*Moswi6* mutant (Fig. 4C).

To evaluate whether the decreased laccase activity was caused by reduced transcription of laccase genes, we examined the transcription of MGG_11608 and MGG_13464 using quantitative RT-PCR. Consistent with other observations, the expression of both laccase genes was reduced in the Δ*Moswi6* mutant (Fig. 4D).

To further test whether enhanced chitin synthesis or compromised melanization contributed to the abnormality in hyphal morphology, we observed the hyphal morphology of the Δ*Moswi6* mutant grown on CM containing 2 mg/mL lysing enzymes or exogenous copper. The results showed that both could rescue the abnormal hyphal morphology of the Δ*Moswi6* mutant (Fig. 5).

Deletion of *MoSWI6* results in abnormal conidia, near loss of penetration and attenuation of pathogenicity

The conidia produced by the Δ*Moswi6* mutant were abnormal, and many (about 40%) had only one septum (Fig. 6A). To investigate the role of MoSwi6 in pathogenesis, conidia were sprayed onto host rice (cv. CO-39) seedlings. The assay showed that the

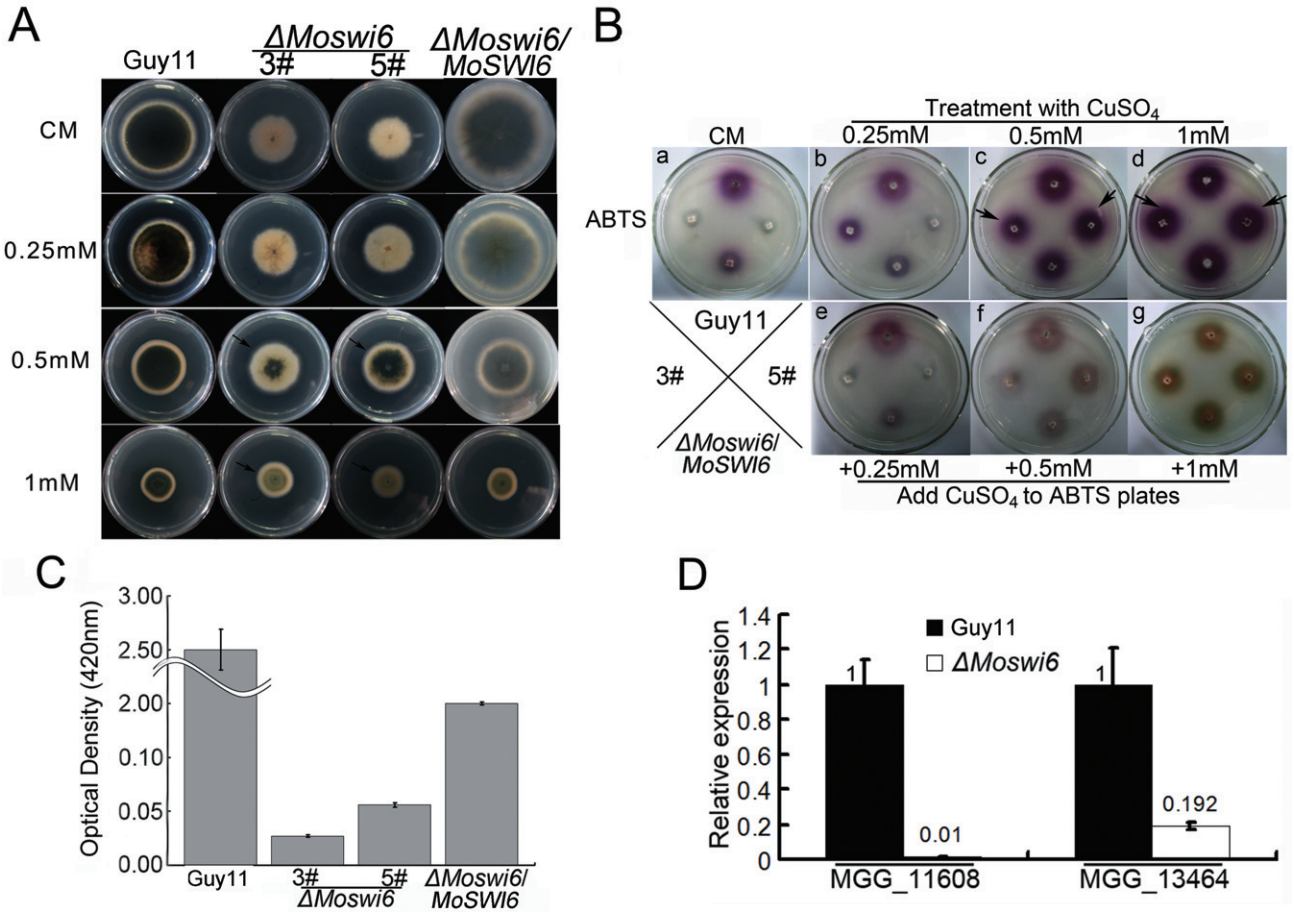

Fig. 4 Laccase activity is reduced in Δ*Moswi6* and can be restored by the addition of $CuSO_4$. (A) After growth for 6 days with Cu^{2+} on complete medium (CM), melanin was restored to the Δ*Moswi6* mutant, particularly on medium containing 0.5–1 mM $CuSO_4$. (B) The Guy11 Δ*Moswi6* mutants (#3 and #5) and the reconstituted (Δ*Moswi6/MoSWI6*) strains were incubated on a CM plate for 6 days (a) and then incubated on a 2,2′-azino-di-3-ethylbenzathiazoline-6-sulphonate (ABTS) (0.2 mM) plate (b–d). After a 6-day treatment with 0.25, 0.5 or 1 mM $CuSO_4$, respectively, the Guy11 Δ*Moswi6* mutants (#3 and #5) and the reconstituted (Δ*Moswi6/MoSWI6*) strains were incubated on an ABTS plate (0.2 mM) for 24 h. (e–g) The Guy11 Δ*Moswi6* mutants (#3 and #5) and the reconstituted (Δ*Moswi6/MoSWI6*) strains were incubated on CM for 6 days and then incubated on an ABTS plate (0.2 mM) supplemented with 0.25, 0.5 and 1 mM $CuSO_4$ for 24 h. (C) Laccase activity absorption value at a wavelength of 420 nm. The laccase activity in the Δ*Moswi6* (#3) mutant was reduced compared with that of the wild-type Guy11. (D) Transcription of putative laccase genes in the Δ*Moswi6* (#3) mutant and wild-type Guy11. The relative abundance of the transcripts compared with the standard condition (wild-type) is displayed as a number. Data represent three independent experiments, each performed three times.

virulence of the Δ*Moswi6* mutant was remarkably reduced. Following inoculation of the Δ*Moswi6* mutant, the rice seedlings exhibited minor lesions in comparison with the major lesions caused by the wild-type strain. In addition, lesions incurred by the Δ*Moswi6* mutant remained restricted, in contrast with the fully expanded necrotic lesions caused by the wild-type strain (Fig. 6B,C). This study demonstrates that the Δ*Moswi6* mutant is attenuated in pathogenicity.

The *Momps1* mutant failed to cause disease because of a defect in penetration of the host (Xu *et al*., 1998). Given that MoSwi6 could be an effector of MoMps1, we examined infection-related morphogenesis using a sensitive penetration assay in onion epidermal cells. About 50% of the Δ*Moswi6* mutant conidia produced abnormal appressoria, which were smaller than those of the wild-type strain (Fig. 6D, panel a, see arrows). In addition, about 50% of the conidia from the Δ*Moswi6* mutant generated more than one germ tube on the surface of the onion epidermis, but failed to penetrate (Fig. 6D, panel b). Moreover, we performed a penetration assay on the rice leaf sheath, according to the method described by Guo *et al*. (2010) and Zhang *et al*. (2011a). As a result, most of the appressoria produced by the Δ*Moswi6* mutant failed to penetrate the rice cell 48 h after inoculation, in contrast with the wild-type infectious hyphae, which actively grew within the primary infected and neighbouring cells (Fig. 6E).

To further explore the contributory factors to the penetration defects in the Δ*Moswi6* mutant, appressoria turgor was measured with an incipient cytorrhysis assay (Zhang *et al*., 2010a). More than 60% of appressoria in the Δ*Moswi6* mutant failed to

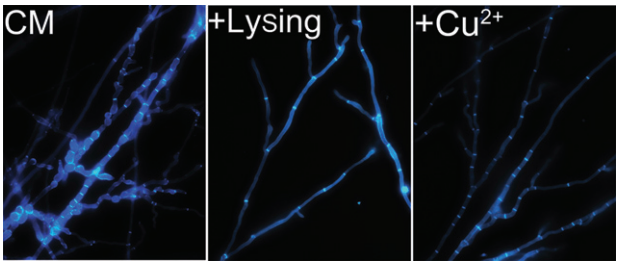

Fig. 5 The abnormal hyphal morphology of the Δ*Moswi6* mutant was rescued by the addition of cell wall lysing enzymes or $CuSO_4$. All strains were stained with calcofluor white and fluorescence was mainly distributed on the apex of hyphae and septa. Mycelial morphology was determined under a microscope after the Δ*Moswi6* mutants had been grown for 2 days on complete medium (CM) (control) or after the addition of cell wall lysing enzymes or exogenous copper on overlaid microscope slides.

collapse, even in 5 M glycerol, compared with the near 100% collapse rate of the wide-type appressoria (Fig. 6F), indicating that MoSwi6 plays a role in turgor.

MoSwi6 plays a role downstream of the Momps1 cascade

In *S. cerevisiae*, the Slt2 pathway regulates the response to oxidative stresses, in additional to cell wall integrity (Krasley *et al*., 2006). Therefore, we tested whether the *Moswi6* mutant has an altered tolerance to oxidative stress. Indeed, mycelial growth of the Δ*Moswi6* mutant was severely inhibited on CM containing 2–5 mM H_2O_2 (Fig. 7A,B). We postulated that the sensitivity of the Δ*Moswi6* mutant to H_2O_2 was probably caused by a loss of the ability to detoxify extracellular H_2O_2. Measurement using extracellular culture filtrates revealed a total loss of peroxidase activity in the Δ*Moswi6* mutant (Fig. 7C). Moreover, transcription examination showed that four of the five peroxidase genes were down-regulated (Fig. 7D). Collectively, these findings indicate that the reduced sensitivity of the Δ*Moswi6* mutant to extracellular H_2O_2 is caused by a low level of peroxidase activity, and that MoSwi6 may play a role in the degradation of extracellular reactive oxygen species (ROS), a factor also important in the pathogenicity of *M. oryzae*.

DISCUSSION

We identified MoSwi6, a homologue of *S. cerevisiae* Swi6, as a putative APSES transcription factor which exhibits important regulatory functions for hyphal growth, conidiation, appressorium-mediated host penetration, cell wall integrity and pathogenicity of *M. oryzae*. Genetic analysis suggested that MoSwi6 functions as an effector of the MoMps1-mediated signalling pathway.

MoSwi6 is necessary for hyphal morphogenesis

Fungal APSES transcription factors are involved in the regulation of morphological changes (Borneman *et al*., 2002; Ohara and Tsuge, 2004) and the expression of genes encoding metabolic enzymes (Doedt *et al*., 2004) and cell wall proteins (Sohn *et al*., 2003). Thus, the morphological defects observed in the Δ*Moswi6* mutant suggest a conserved role of an APSES transcription factor in hyphal morphogenesis. Our observations of enhanced chitin synthesis and compromised melanization resulting in breached cell wall integrity underlie the causes of the morphological defects. Consequently, modification of the cell wall structure by a reduction in chitin content, addition of lysing enzymes or enhancement of melanization by the addition of exogenous copper was able to restore normal hyphal morphology to the Δ*Moswi6* mutants. This finding indicates that MoSwi6 is required for hyphal morphogenesis through the regulation of the genes involved in the biosynthesis of chitin and melanin.

MoSwi6 is a functional homologue of *S. cerevisiae* Swi6 and plays a role downstream of MoMps1 signalling

MoSwi6 contains a conserved APSES domain and four ANK repeats, whereas *S. cerevisiae* Swi6 contains only ANK repeats. Interestingly, proteins of other fungal Swi6 homologues all contain the APSES domain, suggesting that this type of transcription factor may evolve to exhibit novel functions in filamentous fungi. The Δ*Moswi6* mutants showed reduced vegetative growth; however, a similar observation was not found in the *AnSwi6* mutants of *Aspergillus nidulans* (Fujioka *et al*., 2007). Thus, there may also exist functional distinction among Swi6 transcription factors in filamentous fungi. As *S. cerevisiae* Swi6 appears as a downstream transcription factor of the Slt2 MAPK, the interaction between MoSwi6 and MoMps1 may indicate that MoSwi6 and MoMps1 function in an analogous fashion. MoMps1 is important in conidiation and infection (Xu *et al*., 1998) and, indeed, MoSwi6 exhibits similar functions. Moreover, MoSwi6 interacts with MoMps1 in both *in vivo* and *in vitro* environments.

Incidentally, MoMig1, a homologue of *S. cerevisiae* Rlm1 functioning downstream of Slt2, exhibits shared as well as distinct functions with MoSwi6. Deletion of *MoMIG1* had no effect on either growth or appressorium formation, but blocked the differentiation of secondary infectious hyphae (Mehrabi *et al*., 2008). The Δ*Momig1* mutant also differs from the Δ*Moswi6* (and Δ*Momps1*) mutant in colony morphology and conidiation. However, both MoSwi6 and MoMig1 failed to develop infectious hyphae on the host plant.

The important role of MoMps1 signalling in the growth and development of *M. oryzae* is well documented. Here, we characterized that MoSwi6 is a novel transcription factor functioning in

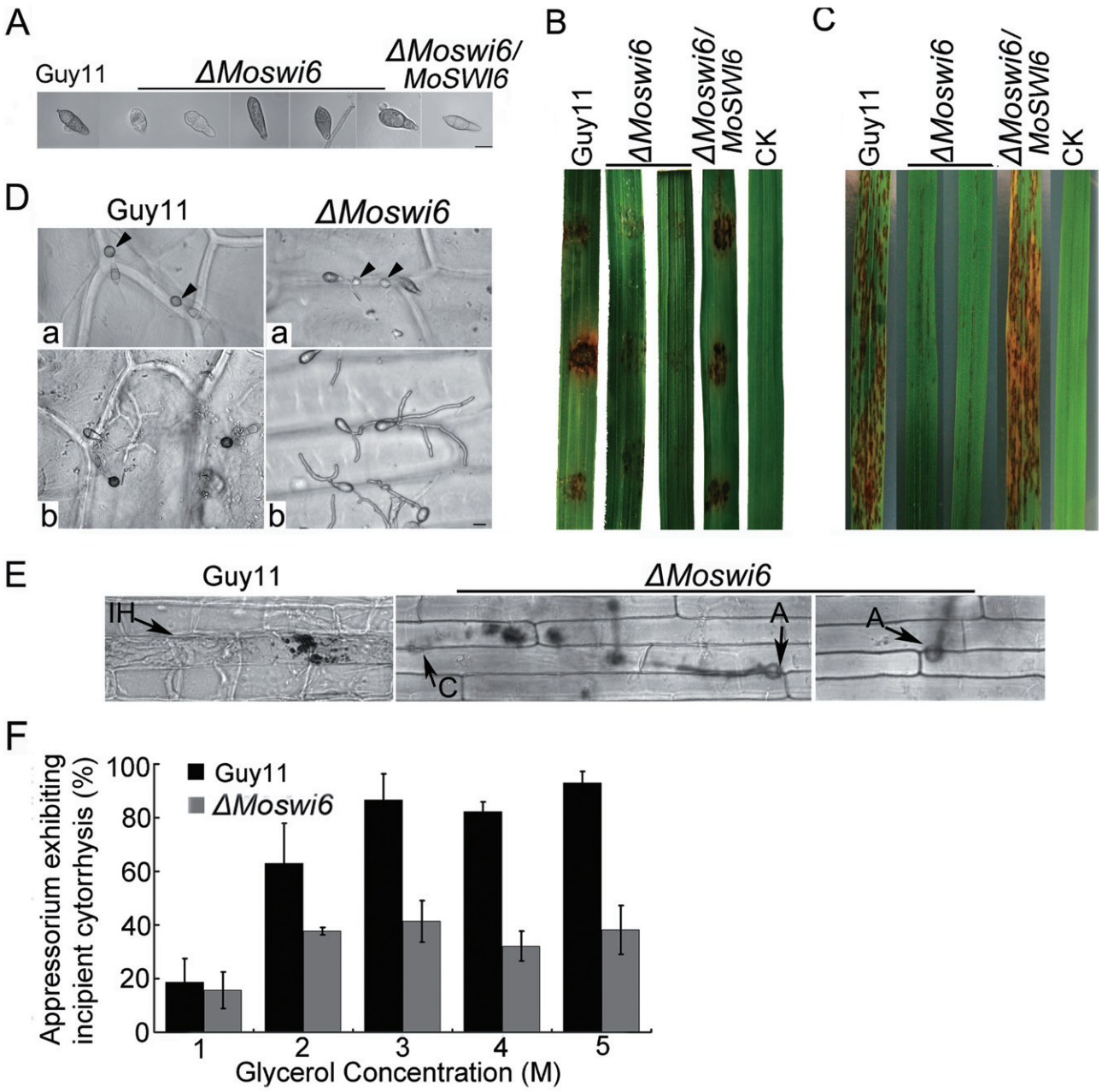

Fig. 6 Morphological observations of conidia, cuticle penetration and pathogenicity assays on rice cultivar *Oryza sativa* cv. CO-39. (A) The Δ*Moswi6* mutants produced conidia with abnormal morphology. Placing (B) and spraying (C) assays on rice leaves with the wild-type strain, Δ*Moswi6* mutants and the reconstituted (Δ*Moswi6/MoSWI6*) strains with water as a negative control. The pathogenicity assay showed that the virulence of the Δ*Moswi6* mutant was remarkably reduced. (D) The Δ*Moswi6* mutant conidia produced abnormal appressoria, which displayed little or no melanin, and were smaller in size than those of the wild-type (a). Most Δ*Moswi6* conidia, except those produced by appressoria, generated very long germ tubes, which adsorbed onto the onion epidermal surface, but failed to penetrate (b). (E) Penetration assay with conidial suspensions on host rice leaf sheath showed the same result as on the onion epidermis. Infectious hyphae were microscopically photographed 48 h after inoculation. A, appressorium; C, conidium; IH, infectious hyphae. (F) Quantification of collapsed appressoria. At least 100 appressoria were observed at each glycerol concentration, and the total numbers of collapsed appressoria were counted.

the MoMps1 signalling pathway and that MoSwi6 is also involved in the regulation of pathogenicity. MoSwi6 negatively regulated chitin synthase expression, as a higher expression of these genes was found in the Δ*Moswi6* mutant. Additional evidence also supports the proposition that MoSwi6 is an important oxidative stress response regulator and plays a positive role in the regulation of extracellular peroxidases. These findings further the understanding of the diverse roles played by the conserved MoMps1 MAPK

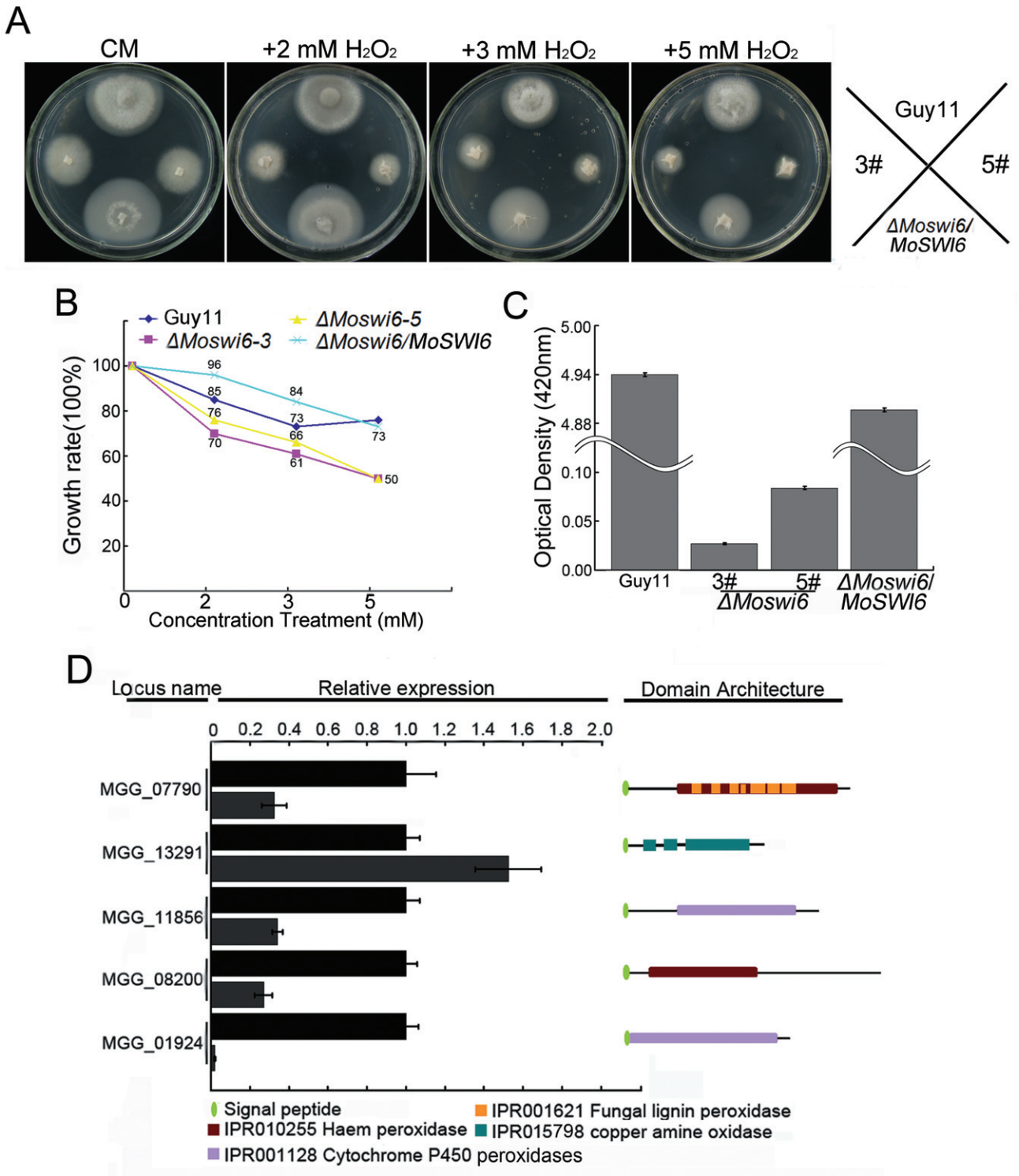

Fig. 7 Δ*Moswi6* mutants were sensitive to H_2O_2. (A) The Δ*Moswi6* mutants (#3 and #5), wild-type and reconstituted (Δ*Moswi6/MoSWI6*) strains were incubated on complete medium (CM) plates supplemented with 2, 3 or 5 mM H_2O_2 for 6 days. (B) The Δ*Moswi6* mutants were sensitive to H_2O_2. Growth rate = 1 − [(diameter on CM − diameter on CM with H_2O_2)/diameter on CM]. (C) Peroxidase activity was measured using the 2,2′-azino-di-3-ethylbenzathiazoline-6-sulphonate (ABTS) oxidizing test under the condition in which H_2O_2 was supplemented. (D) Expression profiles of five peroxidase genes with a signal peptide domain and their predicted peroxidases. Locus names, relative expression characteristics and domain architecture are displayed. InterPro terms and signal peptides are as indicated.

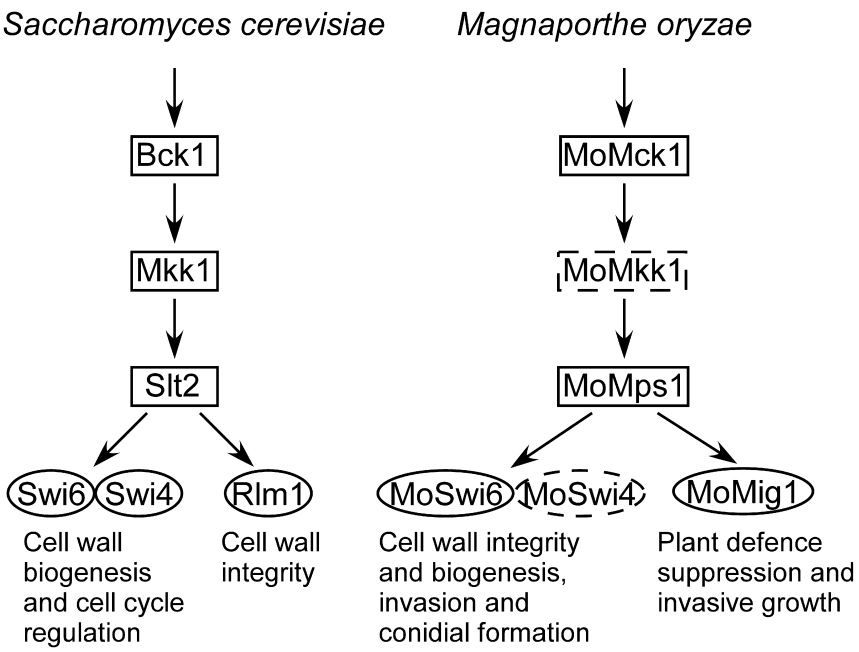

Fig. 8 Comparison of mitogen-activated protein kinase (MAPK) signalling between *Magnaporthe oryzae* MoMps1–MoSwi6 and *Saccharomyces cerevisiae* Slt2–Swi6. Schematic illustration of MoSwi6 functioning downstream of MoMps1 to regulate mycelial and conidial morphogenesis, cell wall integrity and virulence in *M. oryzae*. MoMps1 is thought to interact with MoSwi6, and MoMig1 may also function downstream of MoMps1 independent of MoMps1 (Jeon *et al*., 2008; Mehrabi *et al*., 2008) (indicated by the dotted outline). The MoMps1–MoSwi6 pathway mimics the Slt2–Swi6 pathway of *S. cerevisiae* (Iyer *et al*., 2001; Levin, 2005; Watanabe *et al*., 1995).

signalling in *M. oryzae*. A summarizing model for MoMps1–MoSwi6/MoMig1 function and its comparison with *S. cerevisiae* Slt2–Swi6 is presented in Fig. 8.

Effects of MoSwi6 on pathogenicity

There are two possible explanations for the significantly reduced pathogenicity of the Δ*Moswi6* mutants. First, the loss of appressoria penetration ability resulting from turgor changes may partly contribute to the loss of pathogenicity. In glycerol solutions, the appressoria turgor pressure of the Δ*Moswi6* mutant was reduced significantly, which indicates that the collapse of appressoria was similar to that caused by the presence of hyperosmotic glycerol. The defect of the Δ*Moswi6* mutant with regard to infectious hyphal growth also mimics that of other known nonpathogenic mutants of *M. oryzae*. For example, the Δ*Momac1* and Δ*Momgb1* mutants lacking MoMac1 and MoMgb1 of the PMK1 MAPK pathway, respectively, were defective in appressorium formation (Park *et al*., 2006; Zhao *et al*., 2005). The transcription factor MoMst12 is required for the formation of the penetration peg, although it is dispensable for appressorium formation (Park *et al*., 2004). The Δ*Moatg8* mutant is also defective in appressorium turgor generation and infectious growth (Veneault-Fourrey *et al*., 2006). Finally, the Δ*Mopls1* mutant is defective in appressoria penetration and the development of infectious hypha-like structures in cellophane membranes (Clergeot *et al*., 2001). Second, in fungi such as *N. crassa*, singlet oxygen is generated at the start of conidial germination (Hansberg *et al*., 1993), whereas, in *Podospora anserina*, ROS is required for ascospore germination (Malagnac *et al*., 2004). The loss of MoSwi6 function may have interfered with the ability of this fungus to suppress certain plant defence responses or to colonize living host tissues. Conversely, as fungal pathogens possess counter-defence mechanisms against plant ROS-mediated resistance in order to successfully colonize and reproduce in host plants, the secreted peroxidases may be an important component for the fungal pathogens to detoxify host-derived ROS (Chi *et al*., 2009; Guo *et al*., 2010, 2011; Molina and Kahmann, 2007). The lost pathogenicity of the Δ*Moswi6* mutant may be caused by its hypersensitivity to oxidative stress as a result of the reduced expression and activity of peroxidase genes.

EXPERIMENTAL PROCEDURES

Fungal strains, medium and growth conditions

Magnaporthe oryzae Guy11 was used as the wild-type strain. All strains were cultured on CM (Talbot *et al*., 1993) or minimal medium (MM) (6 g $NaNO_3$, 0.52 g KCl, 0.52 g $MgSO_4$, 1.52 g KH_2PO_4, 10 g glucose and 0.5% biotin in 1 L of distilled water) with or without additional agents for 3–6 days at 28 °C to assess growth and colony characteristics (Zhang *et al*., 2011b). OMA medium (30 g oatmeal and 10 g agar in 1 L of distilled water) and SDC medium were also used. Mycelia were harvested from liquid CM after 2 days of growth and used for genomic DNA and total RNA extractions. To promote conidiation, strains were cultured on SDC medium for 1 week in the dark, followed by 3 days of continuous illumination.

Cloning and sequencing of the *MoSWI6* gene

A cDNA fragment containing a full ORF of the *MoSWI6* gene was cloned from Guy11 cDNA using primers FL3157 and FL2911. The amplified

products were cloned into pMD19 T-vector (TaKaRa, Dalian, China) to generate pMD-*MoSWI6*. The sequence was verified by sequencing.

Targeted gene disruption and complementation of the Δ*Moswi6* mutant

The targeted gene deletion vector pMD-*MoSWI6*KO was constructed by inserting the *HPH* gene expression cassette, which encodes hygromycin phosphotransferase, into the two flanking sequences of the *MoSWI6* gene according to the methods of Zhang *et al*. (2009). An *Eco*RV restriction site was incorporated into primers FL2791 and FL2792. The *HPH* gene expression cassette fragment was prepared by PCR with Primer STAR (TaKaRa) using *Pfu* Taq DNA polymerase from the plasmid pCB1003 with primer pairs FL1111/FL1112, and was then inserted into the *Eco*RV site of pMD-Moswi6 to generate the final construct pMD-*MoSWI6*KO. A 3.4-kb fragment containing the deleted gene was amplified using pMD-*MoSWI6*KO as template with primers FL2790/FL2793, purified by gel electrophoresis and used to transform protoplasts of *M. oryzae* strain Guy11. All amplified fragments were verified by sequencing. Protoplast-mediated transformation was performed following the method of Talbot *et al*. (1993).

To reconstitute the Δ*Moswi6* mutant, a fragment of approximately 4.6 kb was amplified with primers FL3233 and FL3234, which contained the promoter region and the entire ORF, and was inserted into the vector pCB1532 containing a sulphonylurea (*SUR*) resistance gene. After sequence verification, the construct was used to transform the protoplasts.

Southern blotting and RT-PCR

For Southern blotting analysis, DNA digested with *Sma*I, *Eco*RV and *Eco*RI, respectively, was separated and transferred onto a positively charged nylon transfer membrane. The labelled probe was amplified from genomic DNA by the primer pair FL3157 and FL2911. For Southern hybridization analysis of Δ*Moswi6* mutants, genomic DNA was digested with *Eco*RI. Labelled probe A was amplified from genomic DNA using the primers FL3157 and FL3197. Labelled probe B was constructed from *HPH* fragments amplified from plasmid pCB1003 by primers FL1111 and FL1112. The hybridization was carried out in accordance with the manufacturer's instructions for digoxigenin high-prime DNA labelling and the detection starter kit I (Roche, Penzberg, Germany).

Total RNA samples were isolated using NucleoSpin RNAII (Macherey-Nagel, Bethlehem, PA, USA). All RNA used for RT-PCR was treated with DNase I (TaKaRa) prior to cDNA synthesis to exclude DNA contamination. First-strand cDNA was synthesized from the treated RNA using the synthesis system of M-MLV Reverse Transcriptase (Invitrogen, Shanghai, China) and oligo(dT) 15 primers (TaKaRa). Semi-quantitative RT-PCR was performed. A 0.3-kb PCR fragment for the *actin* gene (MGG_03982) was amplified as an internal control using primers FL474 and FL475. The transcript analysis of *MoSWI6* was performed using primers FL3157 and FL3197. The internal control was amplified by PCR of 26 cycles, and *MoSWI6* was amplified by PCR of 30 cycles. All RT-PCRs were repeated at least three times.

Establishment of an interaction between MoSwi6 and Momps1 by yeast two-hybrid screening and co-IP

Yeast two-hybrid assay with MoSwi6 as the bait and MoMps1 as the prey was performed. *MoSWI6* and *MoMPS1* cDNAs were amplified with primer pairs FL3347/FL3348 and FL3349/FL3350, respectively. The amplified products were cloned into the pGBKT7 and pGADT7 vectors (BD Biosciences Clontech, Oxford, UK), respectively. After sequence verification, they were transformed into yeast AH109 strain following the manufacturer's recommended protocol (BD Biosciences Clontech). Yeast transformants grown on synthetic medium minus leucine and tryptophan (SD–Leu–Trp) were transferred to synthetic medium minus leucine, tryptophan, adenine and histidine (SD–Leu–Trp–Ade–His). The interaction was further examined by performing β-galactosidase activity using 5-Bromo-4-chloro-3-indolyl β-D-galactopyranoside (X-gal) (80 μg/L). The interaction between pGBKT7-53 and pGADT7-T was used as the positive control. The interactions between pGBKT7-Lam and pGADT7-T, BD (pGBKT7)-MoSwi6 and AD (pGADT7), BD and AD-MoMps1, and AD- and BD-empty vectors were used as negative controls

The sequences of the primers used in this study are listed in Table S2 (see Supporting Information).

PCR products containing *MoSWI6* or *MoMPS1* and its native promoter were amplified with primers FL8764/FL8765 and FL8768/FL8769, respectively. The *MoMPS1*-3xFLAG and *MoSWI6*-GFP constructs were generated with the yeast gap repair approach (Bourett *et al*., 2002; Bruno *et al*., 2004) and confirmed by sequencing. The resulting fusion constructs were co-transformed into protoplasts of 70-15. Transformants expressing the *MoMPS1*-3xFLAG and *MoSWI6*-GFP constructs were identified by PCR and confirmed by Western blot analysis with an anti-FLAG antibody (Sigma-Aldrich, St. Louis, MO, USA). For co-IP assays, total proteins were isolated from vegetative hyphae as described by Bruno *et al*. (2004) and incubated with anti-FLAG M2 beads (Sigma-Aldrich). Western blots of proteins eluted from the M2 beads were detected with the anti-GFP and anti-FLAG antibodies.

Assays for vegetative growth

Squares of mycelia (2 mm × 2 mm in size) were picked from 6-day-old CM plates and incubated on the centre of 60-mm Petri dishes containing various media (CM, V8, OMA, SDC, MM), supplemented with or without different compounds, and cultured at 28 °C in the dark. The radial growth of mycelia was measured after incubation for 6 days. All the experiments were repeated three times with three replicates each time.

Morphological observation of conidia and assays for appressorium cuticle penetration and turgor

Conidia were harvested from 10-day-old cultures, filtered through three layers of lens paper and observed with an Olympus BH-2 microscope (Olympus, Tokyo, Japan). The conidial suspensions for each treatment were prepared as described above and resuspended at a concentration of 5×10^4 spores/mL in sterile water. Droplets (20 μL) of the suspensions were placed on strips of onion epidermis, incubated under humid conditions at room temperature for 24 h and observed microscopically for the elaboration of penetration hyphae. The penetration assay on rice leaf sheath has been described previously (Guo *et al*., 2010; Zhang *et al*., 2011a). The appressorium turgor was measured using an incipient cytorrhysis (cell collapse) assay and a 1–5 M glycerol solution (Howard *et al*., 1991). Droplets (20 μL) of the conidial suspension (5×10^4 spores/mL) were placed on plastic coverslips and incubated in a humid chamber for 24 h at room

temperature. The water surrounding the conidia was removed carefully and then replaced with an equal volume (20 μL) of glycerol at concentrations ranging from 1 to 5 M. The number of appressoria that had collapsed after 10 min was recorded (Zhang *et al*., 2009). The experiments were repeated three times, and at least 100 appressoria were observed for each replicate.

Pathogenicity assay

For pathogenicity assay, we used the leaves from 2-week-old seedlings of the blast-susceptible rice variety CO-39. To induce conidia production, mycelia were incubated on SDC medium at 28 °C in the dark for 10 days, followed by a constant 3–4 days of illumination. For the cut-leaf assay, conidia were suspended to 1×10^5 spores/mL using a haemocytometer. A 30-μL droplet was placed onto the upper side of the cut leaves maintained on 1.5% (w/v) water agar plates. The results were observed after 3–5 days of incubation at 25 °C. For spray inoculation, conidia were suspended to 5×10^4 spores/mL in sterile water supplemented with 0.2% (w/v) gelatin. Then, 3 mL of the conidial suspensions from each treatment were sprayed evenly onto the plants with a sprayer. The inoculated plants were kept in a growth chamber at 25 °C and 90% humidity in the dark for the first 24 h, followed by a 12 h/12 h light/dark cycle exposure. We observed the progression of lesion development daily, documenting lesion growth with photographs and counting them 7–10 days post-inoculation (Zhang *et al*., 2010a, b).

Light microscopy to observe hyphal morphology

Calcofluor white has been used to stain newly synthesized fungal cell wall polymers (Mitchison and Nurse, 1985). To study hyphal morphology, the strains were grown on microscope slides that carried an overlay of CM agar. After incubation for 2 days in a humid chamber at 28 °C, the cell wall and septum of hyphae were dyed by calcofluor white (Sigma-Aldrich) staining, as described by Harris *et al*. (1994). The hyphae were observed with an Olympus BH-2 microscope.

Quantitative RT-PCR

Quantitative PCR was performed using an ABI 7300 real-time PCR system according to the manufacturer's instructions. The quantitative PCR was in a volume of 20 μL containing 2 μL of reverse transcription product, 10 μL of SYBR® Premix Ex Taq™ (2 μL), 0.4 μL ROX Reference Dye (50×) (SYBR® PrimeScript™ RT-PCR Kit, TaKaRa) and 0.4 μL of each primer (10 μM). A 0.2-kb PCR fragment for the *actin* gene (MGG_03982) was amplified as an internal control using the primers FL4362 and FL4363.

Primers for the transcript analyses of seven chitin synthase genes (MGG_01802, MGG_04145, MGG_09551, MGG_06064, MGG_09962, MGG_13013 and MGG_13014) are listed in Table S3 (see Supporting Information).

Transcript analyses of the laccase encoding genes MGG_11608 and MGG_13464 were performed using the primer pairs FL4368/FL4369 and FL4370/FL4371, respectively. The transcript analysis of *MoBUF1* (MGG_02252) and *MoRSY1* (MGG_05059) genes, involved in melanin biosynthesis, was performed using primers FL4712/FL4713 and FL4710/FL4711, respectively. Transcript analyses of genes MGG_07790, MGG_13291, MGG_11856, MGG_08200 and MGG_01924, which contain signal peptides and encode predicted peroxidases, are also shown in Table S3.

Bioinformatics

The full sequence of *MoSWI6* was downloaded from http://www.broadinstitute.org/annotation/genome/magnaporthe_grisea/MultiHome.html. Swi6 sequences of different organisms were obtained from GenBank (http://www.ncbi.nlm.nih.gov/BLAST) using the BLAST algorithm (McGinnis and Madden, 2004). Sequence alignments were performed using the CLUSTAL_W program (Thompson *et al*., 1994), and the phylogenetic tree was viewed using the Mega3.0 Beta program (Kumar *et al*., 2004). The signal peptide of peroxidases and laccases was predicted by SignalP v3.0. The domain architecture was provided by the European Bioinformatics Institute (EBI) (http://www.ebi.ac.uk/) online database.

ACKNOWLEDGEMENTS

We thank Z. Y. Wang of Zhejiang University, Hangzhou, China for plasmids pCB1532 and pCB1003. We gratefully acknowledge funding from the National Basic Research Program of China (Grant No. 2012CB114000 to ZGZ), Natural Science Foundations of China (Grant No. 30971890 to XBZ), the Fundamental Research Funds for the Central Universities (KYZ201105) and the Project of Jiangsu of China [Grant No. Sx(2009)54 to XBZ]. Research in PW's laboratory was supported by funds from the National Institutes of Health (NIH), Bethesda, MD, USA (AI054958 and AI074001).

REFERENCES

Aramayo, R., Peleg, Y., Addison, R. and Metzenberg, R. (1996) Asm-1+, a *Neurospora crassa* gene related to transcriptional regulators of fungal development. *Genetics*, **144**, 991–1003.

Borneman, A.R., Hynes, M.J. and Andrianopoulos, A. (2002) A basic helix–loop–helix protein with similarity to the fungal morphological regulators, Phd1p, Efg1p and StuA, controls conidiation but not dimorphic growth in *Penicillium marneffei*. *Mol. Microbiol.* **44**, 621–631.

Bourett, T.M., Sweigard, J.A., Czymmek, K.J., Carroll, A. and Howard, R.J. (2002) Reef coral fluorescent proteins for visualizing fungal pathogens. *Fungal Genet. Biol.* **37**, 211–220.

Bruno, K.S., Tenjo, F., Li, L., Hamer, J.E. and Xu, J.R. (2004) Cellular localization and role of kinase activity of *PMK1* in *Magnaporthe grisea*. *Eukaryot. Cell*, **3**, 1525–1532.

Caracuel-Rios, Z. and Talbot, N.J. (2007) Cellular differentiation and host invasion by the rice blast fungus *Magnaporthe grisea*. *Curr. Opin. Microbiol.* **10**, 339–345.

Chi, M.H., Park, S.Y., Kim, S. and Lee, Y.H. (2009) A novel pathogenicity gene is required in the rice blast fungus to suppress the basal defenses of the host. *PLoS Pathog.* **5**, e1000401.

Cid, V.J., Durán, A., del Rey, F., Snyder, M.P., Nombela, C. and Sánchez, M. (1995) Molecular basis of cell integrity and morphogenesis in *Saccharomyces cerevisiae*. *Microbiol. Rev.* **59**, 345–386.

Clergeot, P.H., Gourgues, M., Cots, J., Laurans, F., Latorse, M.P., Pepin, R., Tharreau, D., Notteghem, J.L. and Lebrun, M.H. (2001) *PLS1*, a gene encoding a tetraspanin-like protein, is required for penetration of rice leaf by the fungal pathogen *Magnaporthe grisea*. *Proc. Natl. Acad. Sci. USA*, **98**, 6963–6968.

D'Souza, C.A. and Heitman, J. (2001) Conserved cAMP signaling cascades regulate fungal development and virulence. *FEMS Microbiol. Rev.* **25**, 349–364.

Doedt, T., Krishnamurthy, S., Bockmuhl, D.P., Tebarth, B., Stempel, C., Russell, C.L., Brown, A.J. and Ernst, J.F. (2004) APSES proteins regulate morphogenesis and metabolism in *Candida albicans*. *Mol. Biol. Cell*, **15**, 3167–3180.

Dou, X.Y., Wang, Q., Qi, Z.Q., Song, W.W., Wang, W., Guo, M., Zhang, H.F., Zhang, Z.G., Wang, P. and Zheng, X.B. (2011) MoVam7, a conserved SNARE involved in vacuole assembly, is required for growth, endocytosis, ROS accumulation, and pathogenesis of *Magnaporthe oryzae*. *PLoS ONE*, **6**, e16439.

Ebbole, D.J. (2007) *Magnaporthe* as a model for understanding host–pathogen interactions. *Annu. Rev. Phytopathol.* **45**, 437–456.

Fujioka, T., Mizutani, O., Furukawa, K., Sato, N., Yoshimi, A., Yamagata, Y., Nakajima, T. and Abe, K. (2007) MpkA-dependent and -independent cell wall integrity signaling in *Aspergillus nidulans*. *Eukaryot. Cell*, **6**, 1497–1510.

Guo, M., Guo, W., Chen, Y., Dong, S.M., Zhang, X., Zhang, H.F., Song, W.W., Wang, W., Wang, Q., Lv, R.L., Zhang, Z.G., Wang, Y.C. and Zheng, X.B. (2010) The basic leucine zipper transcription factor Moatf1 mediates oxidative stress responses and is necessary for full virulence of the rice blast fungus *Magnaporthe oryzae*. *Mol. Plant–Microbe Interact.* **23**, 1053–1068.

Guo, M., Chen, Y., Du, Y., Dong, Y.H., Guo, W., Zhai, S., Zhang, H.F., Dong, S.M., Zhang, Z.G., Wang, Y.C., Wang, P. and Zheng, X.B. (2011) The bZIP transcription factor MoAP1 mediates the oxidative stress response and is crucial for pathogenicity of the rice blast fungus *Magnaporthe oryzae*. *PLoS Pathog.* **7**, e1001302.

Hansberg, W., de Groot, H. and Sies, H. (1993) Reactive oxygen species associated with cell differentiation in *Neurospora crassa*. *Free Radic. Biol. Med.* **14**, 287–293.

Harris, S.D., Morrell, J.L. and Hamer, J.E. (1994) Identification and characterization of *Aspergillus nidulans* mutants defective in cytokinesis. *Genetics*, **136**, 517–532.

Henson, J.M., Butler, M.J. and Day, A.W. (1999) The dark side of the mycelium: melanins of phytopathogenic fungi. *Annu. Rev. Phytopathol.* **37**, 447–471.

Howard, R.J., Ferrari, M.A., Roach, D.H. and Money, N.P. (1991) Penetration of hard substrates by a fungus employing enormous turgor pressures. *Proc. Natl. Acad. Sci. USA*, **88**, 11 281–11 284.

Iyer, V.R., Horak, C.E., Scafe, C.S., Botstein, D., Snyder, M. and Brown, P.O. (2001) Genomic binding sites of the yeast cell-cycle transcription factors SBF and MBF. *Nature*, **409**, 533–538.

Jeon, J., Goh, J., Yoo, S., Chi, M.H., Choi, J., Rho, H.S., Park, J., Han, S.S., Kim, B.R., Park, S.Y., Kim, S. and Lee, Y.H. (2008) A putative MAP kinase kinase kinase, MCK1, is required for cell wall integrity and pathogenicity of the rice blast fungus, *Magnaporthe oryzae*. *Mol. Plant–Microbe Interact.* **21**, 525–534.

Krasley, E., Cooper, K.F., Mallory, M.J., Dunbrack, R. and Strich, R. (2006) Regulation of the oxidative stress response through Slt2p-dependent destruction of cyclin C in *Saccharomyces cerevisiae*. *Genetics*, **172**, 1477–1486.

Kumar, S., Tamura, K. and Nei, M. (2004) MEGA3: integrated software for molecular evolutionary genetics analysis and sequence alignment. *Brief. Bioinform.* **5**, 150–163.

Levin, D.E. (2005) Cell wall integrity signaling in *Saccharomyces cerevisiae*. *Microbiol. Mol. Biol. Rev.* **69**, 262–291.

Malagnac, F., Lalucque, H., Lepere, G. and Silar, P. (2004) Two NADPH oxidase isoforms are required for sexual reproduction and ascospore germination in the filamentous fungus *Podospora anserina*. *Fungal Genet. Biol.* **41**, 982–997.

McGinnis, S. and Madden, T.L. (2004) BLAST: at the core of a powerful and diverse set of sequence analysis tools. *Nucleic Acids Res.* **32**, W20–W25.

Mehrabi, R., Ding, S. and Xu, J.R. (2008) MADS-box transcription factor mig1 is required for infectious growth in *Magnaporthe grisea*. *Eukaryot. Cell*, **7**, 791–799.

Mitchison, J.M. and Nurse, P. (1985) Growth in cell length in the fission yeast *Schizosaccharomyces pombe*. *J. Cell Sci.* **75**, 357–376.

Molina, L. and Kahmann, R. (2007) An *Ustilago maydis* gene involved in H_2O_2 detoxification is required for virulence. *Plant Cell*, **19**, 2293–2309.

Nishimura, M., Fukada, J., Moriwaki, A., Fujikawa, T., Ohashi, M., Hibi, T. and Hayashi, N. (2009) Mstu1, an APSES transcription factor, is required for appressorium-mediated infection in *Magnaporthe grisea*. *Biosci. Biotechnol. Biochem.* **73**, 1779–1786.

Odenbach, D., Thines, E., Anke, H. and Foster, A.J. (2009) The *Magnaporthe grisea* class VII chitin synthase is required for normal appressorial development and function. *Mol. Plant Pathol.* **10**, 81–94.

Ohara, T. and Tsuge, T. (2004) *FoSTUA*, encoding a basic helix–loop–helix protein, differentially regulates development of three kinds of asexual spores, macroconidia, microconidia, and chlamydospores, in the fungal plant pathogen *Fusarium oxysporum*. *Eukaryot. Cell*, **3**, 1412–1422.

Park, G., Bruno, K.S., Staiger, C.J., Talbot, N.J. and Xu, J.R. (2004) Independent genetic mechanisms mediate turgor generation and penetration peg formation during plant infection in the rice blast fungus. *Mol. Microbiol.* **53**, 1695–1707.

Park, G., Xue, C., Zhao, X., Kim, Y., Orbach, M. and Xu, J.R. (2006) Multiple upstream signals converge on the adaptor protein Mst50 in *Magnaporthe grisea*. *Plant Cell*, **18**, 2822–2835.

Roncero, C. (2002) The genetic complexity of chitin synthesis in fungi. *Curr. Genet.* **41**, 367–378.

Sheppard, D.C., Doedt, T., Chiang, L.Y., Kim, H.S., Chen, D., Nierman, W.C. and Filler, S.G. (2005) The *Aspergillus fumigatus* StuA protein governs the up-regulation of a discrete transcriptional program during the acquisition of developmental competence. *Mol. Biol. Cell*, **16**, 5866–5879.

Shindler, J.S., Childs, R.E. and Bardsley, W.G. (1976) Peroxidase from human cervical mucus. The isolation and characterisation. *Eur. J. Biochem.* **65**, 325–331.

Skamnioti, P., Henderson, C., Zhang, Z., Robinson, Z. and Gurr, S.J. (2007) A novel role for catalase B in the maintenance of fungal cell-wall integrity during host invasion in the rice blast fungus *Magnaporthe grisea*. *Mol. Plant–Microbe Interact.* **20**, 568–580.

Sohn, K., Urban, C., Brunner, H. and Rupp, S. (2003) EFG1 is a major regulator of cell wall dynamics in *Candida albicans* as revealed by DNA microarrays. *Mol. Microbiol.* **47**, 89–102.

Song, W.W., Dou, X.Y., Qi, Z.Q., Wang, Q., Zhang, X., Zhang, H.F., Guo, M., Dong, S.M., Zhang, Z.G., Wang, P. and Zheng, X.B. (2010) R-SNARE homolog MoSec22 is required for conidiogenesis, cell wall integrity, and pathogenesis of *Magnaporthe oryzae*. *PLoS ONE*, **5**, e13193.

Talbot, N.J. (2003) On the trail of a cereal killer: exploring the biology of *Magnaporthe grisea*. *Annu. Rev. Microbiol.* **57**, 177–202.

Talbot, N.J., Ebbole, D.J. and Hamer, J.E. (1993) Identification and characterization of *MPG1*, a gene involved in pathogenicity from the rice blast fungus *Magnaporthe grisea*. *Plant Cell*, **5**, 1575–1590.

Tebarth, B., Doedt, T., Krishnamurthy, S., Weide, M., Monterola, F., Dominguez, A. and Ernst, J.F. (2003) Adaptation of the Efg1p morphogenetic pathway in *Candida albicans* by negative autoregulation and PKA-dependent repression of the *EFG1* gene. *J. Mol. Biol.* **329**, 949–962.

Thompson, J.D., Higgins, D.G. and Gibson, T.J. (1994) CLUSTAL W: improving the sensitivity of progressive multiple sequence alignment through sequence weighting, position-specific gap penalties and weight matrix choice. *Nucleic Acids Res.* **22**, 4673–4680.

Tong, X., Zhang, X., Plummer, K.M., Stowell, K.M., Sullivan, P.A. and Farley, P.C. (2007) GcSTUA, an APSES transcription factor, is required for generation of appressorial turgor pressure and full pathogenicity of *Glomerella cingulata*. *Mol. Plant–Microbe Interact.* **20**, 1102–1111.

Tucker, S.L. and Talbot, N.J. (2001) Surface attachment and pre-penetration stage development by plant pathogenic fungi. *Annu. Rev. Phytopathol.* **39**, 385–417.

Valent, B., Farrall, L. and Chumley, F.G. (1991) *Magnaporthe grisea* genes for pathogenicity and virulence identified through a series of backcrosses. *Genetics*, **127**, 87–101.

Veneault-Fourrey, C., Barooah, M., Egan, M., Wakley, G. and Talbot, N.J. (2006) Autophagic fungal cell death is necessary for infection by the rice blast fungus. *Science*, **312**, 580–583.

Wang, Q. and Szaniszlo, P.J. (2007) WdStuAp, an APSES transcription factor, is a regulator of yeast-hyphal transitions in *Wangiella* (*Exophiala*) *dermatitidis*. *Eukaryot. Cell*, **6**, 1595–1605.

Ward, M.P., Gimeno, C.J., Fink, G.R. and Garrett, S. (1995) SOK2 may regulate cyclic AMP-dependent protein kinase-stimulated growth and pseudohyphal development by repressing transcription. *Mol. Cell. Biol.* **15**, 6854–6863.

Watanabe, Y., Irie, K. and Matsumoto, K. (1995) Yeast Rlm1 encodes a serum response factor-like protein that may function downstream of the Mpk1 (Slt2) mitogen-activated protein-kinase pathway. *Mol. Cell. Biol.* **15**, 5740–5749.

Watanabe, Y., Takaesu, G., Hagiwara, M., Irie, K. and Matsumoto, K. (1997) Characterization of a serum response factor-like protein in *Saccharomyces cerevisiae*, Rlm1, which has transcriptional activity regulated by the Mpk1 (Slt2) mitogen-activated protein kinase pathway. *Mol. Cell. Biol.* **17**, 2615–2623.

Xu, J.R., Staiger, C.J. and Hamer, J.E. (1998) Inactivation of the mitogen-activated protein kinase Mps1 from the rice blast fungus prevents penetration of host cells but allows activation of plant defense responses. *Proc. Natl. Acad. Sci. USA*, **95**, 12 713–12 718.

Zhang, H.F., Zhao, Q., Liu, K.Y., Zhang, Z.G., Wang, Y.C. and Zheng, X.B. (2009) *MgCRZ1*, a transcription factor of *Magnaporthe grisea*, controls growth, development and is involved in full virulence. *FEMS Microbiol. Lett.* **293**, 160–169.

Zhang, H.F., Liu, K.Y., Zhang, X., Song, W.W., Zhao, Q., Dong, Y.H., Guo, M., Zheng, X.B. and Zhang, Z.G. (2010a) A two-component histidine kinase, *MoSLN1*, is required for cell wall integrity and pathogenicity of the rice blast fungus, *Magnaporthe oryzae*. *Curr. Genet.* **56**, 517–528.

Zhang, H.F., Liu, K.Y., Zhang, X., Tang, W., Wang, J.S., Guo, M., Zhao, Q., Zheng, X.B., Wang, P. and Zhang, Z.G. (2010b) Two phosphodiesterase genes, *PDEL* and *PDEH*, regulate development and pathogenicity by modulating intracellular cyclic AMP levels in *Magnaporthe oryzae*. *PLoS ONE*, **6**, e17241.

Zhang, H.F., Tang, W., Liu, K.Y., Huang, Q., Zhang, X., Yan, X., Chen, Y., Wang, J.S., Qi, Z.Q., Wang, Z.Y., Zheng, X.B., Wang, P. and Zhang, Z.G. (2011a) Eight RGS and

RGS-like proteins orchestrate growth, differentiation, and pathogenicity of *Magnaporthe oryzae*. *PLoS Pathog.* **7**, e1002450.

Zhang, L.S., Lv, R.L., Dou, X.Y., Qi, Z.Q., Hua, C.L., Zhang, H.F., Wang, Z., Zheng, X.B. and Zhang, Z.G. (2011b) The function of MoGlk1 in integration of glucose and ammonium utilization in *Magnaporthe oryzae*. *PLoS ONE*, **6**, e22809.

Zhao, X., Kim, Y., Park, G. and Xu, J.R. (2005) A mitogen-activated protein kinase cascade regulating infection-related morphogenesis in *Magnaporthe grisea*. *Plant Cell*, **17**, 1317–1329.

SUPPORTING INFORMATION

Additional Supporting Information may be found in the online version of this article:

Fig. S1 Southern blotting analysis of the copy numbers of *MoSWI6* in *Magnaporthe oryzae*. Genomic DNA of wild-type Guy11 was digested with *Sma*I, *EcoR*V and *EcoR*I, respectively, and separated in a 0.7% agarose gel. The DNA was hybridized with *MoSWI6* gene probe amplified with primers FL3157/FL2911.

Fig. S2 Phylogenetic analysis of *Magnaporthe oryzae* Swi6 amino acid sequence with its homologues in other organisms. The neighbour-joining tree (with 1000 bootstrap replicates) of phylogenetic relationships between Swi6 homologues in fungi was constructed with the following results: *M. oryzae* (*Magnaporthe oryzae* XP_365024), *G. zeae* (*Gibberella zeae* XP_384396), *P. anserina* (*Podospora anserina* XP_001903283), *N. crassa* (*Neurospora crassa* XP_962967), *C. globosum* (*Chaetomium globosum* XP_001224444), *B. fuckeliana* (*Botryotinia fuckeliana* XP_001557910), *S. sclerotiorum* (*Sclerotinia sclerotiorum* XP_001590455), *A. nidulans* (*Aspergillus nidulans* XP_664319), *A. niger* (*Aspergillus niger* XP_001391313), *A. fumigatus* (*Aspergillus fumigatus* XP_748947), *A. oryzae* (*Aspergillus oryzae* XP_001817491), *A. terreus* (*Aspergillus terreus* XP_001215548), *C. immitis* (*Coccidioides immitis* XP_001246031), *C. albicans* (*Candida albicans* ACH78334) and *S. cerevisiae* (*Saccharomyces cerevisiae* NP_013283). Evolutionary distances are indicated by the scale bar below.

Fig. S3 Amino acid sequence alignment of APSES domain and ankyrin repeat (ANK repeat) of *Magnaporthe oryzae* with their homologues from other fungi. (A) The amino acid alignment of APSES domains from *M. oryzae* (*Magnaporthe oryzae* XP_365024), *B. fuckeliana* (*Botryotinia fuckeliana* XP_001557910), *G. zeae* (*Gibberella zeae* XP_384396), *N. crassa* (*Neurospora crassa* XP_962967), *C. globosum* (*Chaetomium globosum* XP_001224444), *P. anserina* (*Podospora anserina* XP_001903283), *S. sclerotiorum* (*Sclerotinia sclerotiorum* XP_001590455) and *A. oryzae* (*Aspergillus oryzae* XP_001817491). (B) Alignment of ANK repeats of MoSwi6 and its homologues from other fungi. Identical amino acids are highlighted with a black background and similar amino acids with a grey background.

Fig. S4 Targeted deletion of *MoSWI6* in *Magnaporthe oryzae*. (A) Schematic illustration for *MoSWI6* targeted gene replacement. The organization of the *MoSWI6* locus and the gene deletion vector; the positions and orientations of the primers FL2790 (1), FL2791 (2), FL2792 (3) and FL2793 (4) are labelled with small arrows. The FL2790/FL2793 fragment amplified from the gene deletion vector was purified by gel electrophoresis and used to transform *M. oryzae* Guy11 protoplasts. (B) Mutant transformants were verified by Southern blot analysis. Genomic DNA was digested with *EcoR*I and separated on a 0.7% agarose gel. The DNA was hybridized with probe A, amplified with primers FL3157 and FL3197, and probe B, the 1.4-kb *HPH* fragment, amplified with primers FL1111 and FL1112. (C) Mutant transformants were verified by polymerase chain reaction (PCR). Transformants #3 and #5 were representative mutants. Δ*Moswi6/MoSWI6* was obtained by transformation of #3 Δ*Moswi6* strain with the wild-type *MoSWI6* gene. pMD-*Moswi6*, plasmid of knockout construct; pMD-*Moswi6*/*MoSWI6*, plasmid of complemented construct. (D) Mutants were verified by reverse transcriptase-polymerase chain reaction (RT-PCR). The primers used as an endogenous control were specific to *MoSWI6*, using the same total RNA to the *M. oryzae actin* gene. PCR products were separated on an agarose gel and stained with ethidium bromide. Data represent three independent experiments, each performed three times and yielding similar results.

Fig. S5 Deletion *MoSWI6* resulted in reduced growth on various media. The Δ*Moswi6* mutants displayed retarded growth on CM, OMA, V8, MM and SDC media.

Fig. S6 The expression level of two melanin biosynthesis genes in the wild-type and Δ*Moswi6* mutant. Asterisks indicate significant differences at $P = 0.01$.

Table S1 Effects of stress conditions on the growth-inhibiting rate of Guy11 and Δ*Moswi6* mutants[a]

Table S2 Polymerase chain reaction (PCR) primers used in this study.

Table S3 Quantitative reverse transcriptase-polymerase chain reaction (RT-PCR) primers used in this study.

Please note: Wiley-Blackwell are not responsible for the content or functionality of any supporting materials supplied by the authors. Any queries (other than missing material) should be directed to the corresponding author for the article.